JOURNAL OF VIROLOGY, Sept. 2009, p. 8315–8326 Vol. 83, No. 17
0022-538X/09/$08.00+0 doi:10.1128/JVI.00633-09

Anterograde Spread of Herpes Simplex Virus Type 1 Requires Glycoprotein E and Glycoprotein I but Not Us9[▽]

Helen M. McGraw,† Sita Awasthi,† Jason A. Wojcechowskyj, and Harvey M. Friedman*

Division of Infectious Diseases, Department of Medicine, University of Pennsylvania School of Medicine, Philadelphia, Pennsylvania 19104-6073

Received 26 March 2009/Accepted 9 June 2009

Anterograde neuronal spread (i.e., spread from the neuron cell body toward the axon terminus) is a critical component of the alphaherpesvirus life cycle. Three viral proteins, gE, gI, and Us9, have been implicated in alphaherpesvirus anterograde spread in several animal models and neuron culture systems. We sought to better define the roles of gE, gI, and Us9 in herpes simplex virus type 1 (HSV-1) anterograde spread using a compartmentalized primary neuron culture system. We found that no anterograde spread occurred in the absence of gE or gI, indicating that these proteins are essential for HSV-1 anterograde spread. However, we did detect anterograde spread in the absence of Us9 using two independent Us9-deleted viruses. We confirmed the Us9 finding in different murine models of neuronal spread. We examined viral transport into the optic nerve and spread to the brain after retinal infection; the production of zosteriform disease after flank inoculation; and viral spread to the spinal cord after flank inoculation. In all models, anterograde spread occurred in the absence of Us9, although in some cases at reduced levels. This finding contrasts with gE- and gI-deleted viruses, which displayed no anterograde spread in any animal model. Thus, gE and gI are essential for HSV-1 anterograde spread, while Us9 is dispensable.

Alphaherpesviruses are parasites of the peripheral nervous system. In their natural hosts, alphaherpesviruses establish lifelong persistent infections in sensory ganglia and periodically return by axonal transport to the periphery, where they cause recurrent disease. This life cycle requires viral transport along axons in two directions. Axonal transport in the retrograde direction (toward the neuron cell body) occurs during neuroinvasion and is required for the establishment of latency, while transport in the anterograde direction (away from the neuron cell body) occurs after reactivation and is required for viral spread to the periphery to cause recurrent disease. In addition to anterograde and retrograde axonal transport within neurons, alphaherpesviruses spread between synaptically connected neurons and between neurons and epithelial cells at the periphery (19, 22).

The alphaherpesvirus subfamily includes the human pathogens herpes simplex virus type 1 (HSV-1), HSV-2, and varicella-zoster virus (VZV), as well as numerous veterinary pathogens such as pseudorabies virus (PRV) and bovine herpesviruses 1 and 5 (BHV-1 and BHV-5). The molecular mechanisms that mediate alphaherpesvirus anterograde axonal transport, anterograde spread, and cell-to-cell spread remain unclear. However, many studies of several alphaherpesviruses have indicated that anterograde transport or anterograde spread involves the viral proteins glycoprotein E (gE), glycoprotein I (gI), and Us9 (2, 5, 7, 9, 11, 13, 16, 26, 30, 31, 41, 46, 51, 52).

Glycoproteins E and I are type I membrane proteins that form a heterodimer in the virion membrane and on the surface of infected cells. Although dispensable for the entry of extracellular virus, gE and gI mediate the epithelial cell-to-cell spread of numerous alphaherpesviruses (1, 3, 15, 20, 34, 38, 49, 53, 54). Us9 is a type II nonglycosylated membrane protein with no described biological activity apart from its role in neuronal transport (4, 18, 32). Here, we used several model systems to better characterize the roles of gE, gI, and Us9 in HSV-1 neuronal spread.

Animal models to assess alphaherpesvirus neuronal transport (viral movement within a neuron) and spread (viral movement between cells) include the mouse flank and mouse retina models of infection. In the mouse flank model (Fig. 1A), virus is scratch inoculated onto the depilated flank, where it infects the skin and spreads to innervating sensory neurons. The virus travels to the dorsal root ganglia (DRG) in the spinal cord (retrograde direction) and then returns to an entire dermatome of skin (anterograde spread). The virus also is transported in an anterograde direction from the DRG to the dorsal horn of the spinal cord and subsequently spreads to synaptically connected neurons. The production of zosteriform lesions and the presence of viral antigens in the dorsal horn of the spinal cord both are indicators of anterograde spread in this system. PRV gE and Us9 are required for the production of zosteriform disease, while gI is dispensable (7). In the absence of gE, HSV-1 also fails to cause zosteriform disease. However, unlike PRV, HSV-1 gE is required for retrograde spread to the DRG, so the role of gE in HSV-1 anterograde spread could not be evaluated in the mouse flank model (8, 36, 42).

The mouse retina infection model (Fig. 1B) has the advantage of allowing anterograde and retrograde spread to be studied independently of one another. Virus is delivered to the vitreous body, from which it infects the retina and other structures of the eye. The cell bodies of retinal neurons form the innermost layer of the retina; therefore, the virus infects these neurons directly, and spread from the retina along visual path-

* Corresponding author. Mailing address: 502 Johnson Pavilion, University of Pennsylvania, Philadelphia, PA 19104-6073. Phone: (215) 662-3557. Fax: (215) 349-5111. E-mail: hfriedma@mail.med.upenn.edu.
† H.M.M. and S.A. contributed equally to this work.
▽ Published ahead of print on 1 July 2009.

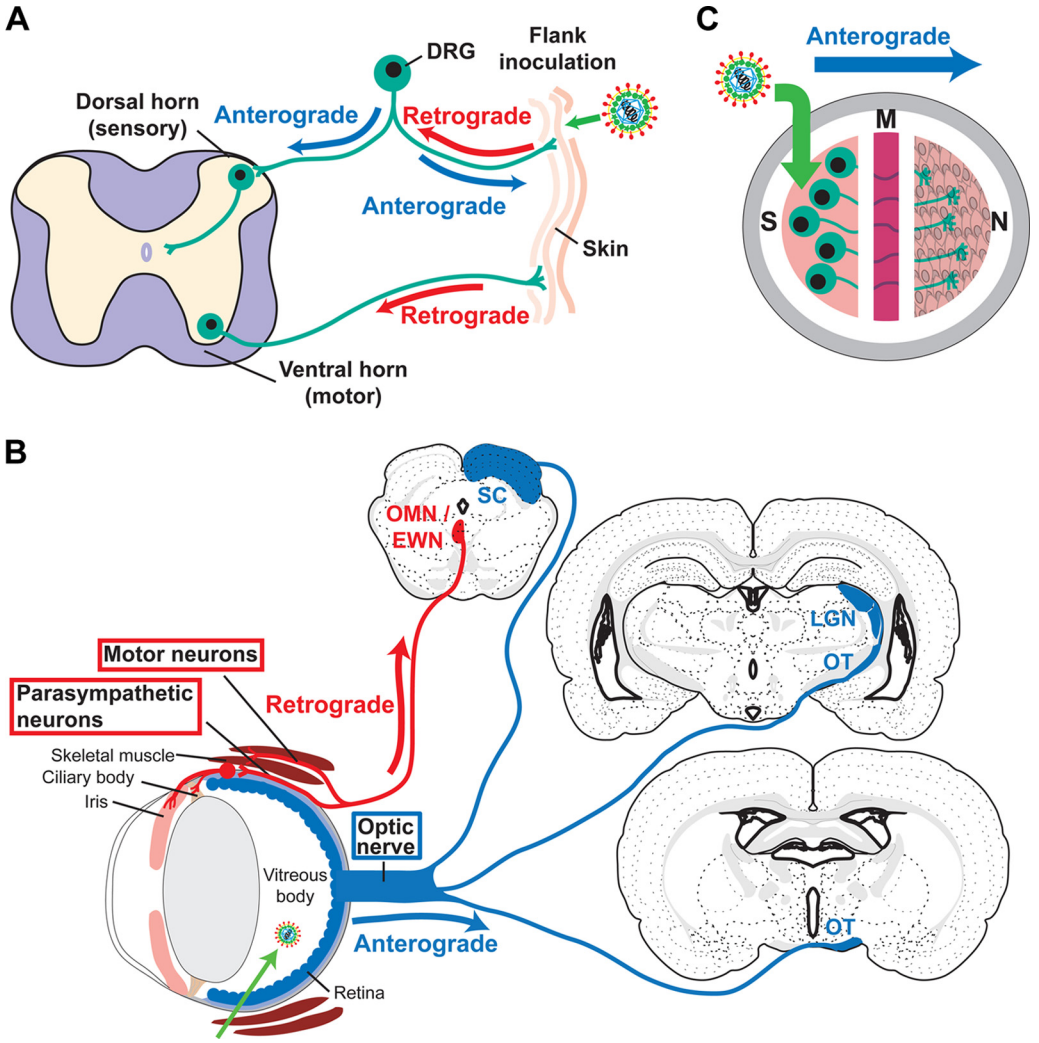

FIG. 1. Model systems to study HSV-1 neuronal spread. (A) Mouse flank model. Virus was scratch inoculated onto the skin, where it replicates, spreads to innervating neurons, and travels in a retrograde direction to the neuron cell body in the DRG. After replicating in the DRG, the virus travels in an anterograde direction back to the skin and into the dorsal horn of the spinal cord. Motor neurons also innervate the skin, allowing virus to reach the ventral horn of the spinal cord by retrograde transport. (B) Mouse retina model. Virus is injected into the vitreous body, from which it infects the retina as well as other structures of the eye, including the ciliary body, iris, and skeletal muscles of the orbit. From the retina, the virus is transported into the optic nerve and optic tract (OT) (anterograde direction) and then to the brain along visual pathways. Anterograde spread is detected in the lateral geniculate nucleus (LGN) and superior colliculus (SC). From the infected ciliary body, iris, and skeletal muscle, the virus spreads in a retrograde direction along motor and parasympathetic neurons and is detected in the oculomotor and Edinger-Westphal nuclei (OMN/EWN). Only first-order sites of spread to the brain are indicated. (Brain images were modified and reproduced from reference 47 with permission from of the publisher. Copyright Elsevier 1992.) (C) Campenot chamber system. Campenot chambers consist of a Teflon ring that divides the culture into three separate compartments. Neurons are seeded into the S chamber and extend their axons into the M and N chambers. Vero cells are seeded into the N chamber 1 day before infection. Virus is added to the S chamber and detected in the N chamber, a measure of anterograde spread.

ways to the brain occurs in an exclusively anterograde direction. In addition, the virus infects the anterior uveal layer of the eye (ciliary body and iris) and skeletal muscles in the orbit. From these tissues, the virus infects innervating parasympathetic and motor neurons and spreads to the brain in a retrograde direction. The localization of viral antigens in specific brain sites indicates whether the virus traveled to the brain along an anterograde or retrograde pathway (21, 25, 26, 39, 44, 51). PRV gE, gI, and Us9 each are essential for anterograde spread to the brain yet are dispensable for retrograde spread (5, 11, 25, 52). Even a strain of PRV lacking all three of these proteins retains retrograde neuronal spread activity (12, 40, 44). In contrast, in the absence of gE, HSV-1 fails to spread to the brain by either the anterograde or retrograde pathway (51).

The Campenot chamber system (Fig. 1C) has the advantage of allowing quantitative measurement of anterograde spread. Sympathetic neurons are cultured in a tripartite ring in which neuron cell bodies are contained in a separate compartment from their neurites. Virus is added to neuron cell bodies in one chamber, and anterograde spread to a separate chamber is measured by viral titers (13, 29, 30, 39, 43). Using this system, gEnull, gInull, and Us9null PRV each were shown to have only

a partial defect in anterograde spread, while a virus lacking all three proteins was totally defective (13).

We sought to quantify the anterograde spread activity of gEnull, gInull, and Us9null HSV-1 using the Campenot chamber system. While gEnull and gInull viruses were completely defective at anterograde spread, we found that a Us9null virus retained wild-type (WT) anterograde spread activity in this system. This observation was unexpected, since others previously had reported that Us9 is required for efficient HSV-1 anterograde transport or spread (26, 41, 46). Therefore, we further characterized the neuronal spread properties of two independent Us9-deleted viruses in the mouse retina and mouse flank models of infection. Our results indicate that gE and gI are essential for HSV-1 anterograde spread, whereas Us9 is dispensable.

MATERIALS AND METHODS

Cells. Vero cells (African green monkey kidney epithelial cells) were propagated in Dulbecco's modified Eagle's medium supplemented with 10 mM HEPES (pH 7.3), 2 mM L-glutamine, 20 μg/ml gentamicin, and 5% heat-inactivated fetal bovine serum.

Viruses. HSV-1 strain NS is a low-passage clinical isolate (23). NS-gEnull contains a LacZ marker replacing gE amino acids 124 to 510 and produces no functional gE protein, while rNS-gEnull is a rescue virus that restores gE expression (36). Us9- and the rescue virus, Us9R, (strain F) were provided by J. H. LaVail, University of California at San Francisco (26). Us9- contains a deletion of nucleotides (nt) 18 to 204, leaving the first 17 nt intact and nt 205 to 270 in an altered reading frame. gInull contains a deletion of the first 886 nt of Us7, leaving the remaining 377 nt in an altered reading frame. gInull and the rescue virus, gInull-R (strain SC16), were provided by T. Minson, Cambridge University (3). Virus stocks were prepared by infecting Vero cells at a multiplicity of infection (MOI) of 0.01 and collecting the infected cells and media when the cytopathic effect reached 100%. Single-step growth curves in dissociated superior cervical ganglia (SCG) neurons and Vero cells were performed as previously described (33). Mouse flank infections were performed using clarified supernatant, while Campenot chamber and mouse retina model infections used virus that was purified on a sucrose gradient and resuspended in phosphate-buffered saline (PBS). Virus titers were determined by plaque assay on Vero cells (33).

Construction of NS-Us9null. A 2-kb fragment of the HSV-1 NS genome spanning the Us9 coding sequence was cloned into a pBluescript SK+ vector. The entire Us9 coding sequence was replaced with an mCherry marker using SOEing PCR, generating plasmid pML71. Linearized pML71 was cotransfected into Vero cells with HSV-1 NS DNA, and cells were overlaid with methylcellulose. Red fluorescent plaques were picked and plaque purified three times to produce NS-Us9null. Candidate plaques were screened by Western blotting for the lack of Us9 expression, and viral DNA was sequenced to confirm the deletion. NS-Us9null was provided by M. G. Lyman and L. W. Enquist, Princeton University.

Antibodies. Anti-HSV-1 (Dako), UP575 (anti-gE), UP1928 (anti-gI), R122 (anti-gD), R118 (anti-gC), NC-1 (anti-VP5), and NC-L anti-light capsid (A capsid) rabbit sera have been described already, as has the anti-gI monoclonal antibody (MAb) Fd69 (17, 24, 27, 28, 50, 51). R122, R118, NC-1, and NC-L sera were provided by G. H. Cohen and R. J. Eisenberg, University of Pennsylvania. NC-L-purified immunoglobulin G was adsorbed against uninfected mouse brain sections prior to use in staining. To prepare UP1990 anti-Us9 serum, Us9 protein was expressed in *Escherichia coli* and separated by sodium dodecyl sulfate-polyacrylamide gel electrophoresis (SDS-PAGE). Us9 expression was confirmed by Western blotting using anti-Us9 rabbit serum provided by B. Roizman, University of Chicago. A 16-kDa band was cut from the gel and used to immunize a rabbit. PSU74 anti-VP22 rabbit serum was provided by R. Courtney, Pennsylvania State University. The anti-actin MAb C4 was obtained from MP Biomedicals. Rat anti-mouse Thy-1.2 (PharMingen) was used as a neuronal cell marker. Secondary antibodies used were Alexa-555 goat anti-rabbit (Invitrogen), Alexa-488 donkey anti-rat (Invitrogen), biotinylated goat anti-rabbit (Sigma), horseradish peroxidase (HRP) anti-mouse (GE Healthcare), and HRP anti-rabbit (GE Healthcare).

Infection of SCG neurons in Campenot chambers. SCG neurons were cultured in Campenot chambers as previously described (Fig. 1C) (10, 13, 14, 33). Briefly, ganglia were dissected from E17 rat embryos and cultured in defined media containing nerve growth factor. Dissociated neurons from half of an SCG were seeded into the soma (S) chamber, resulting in approximately 5,000 neuron cell bodies. The neurons were cultured for 2 to 3 weeks until extensive neurite growth was observed in the neurite (N) chamber. One day prior to infection, the culture medium was changed and the middle (M) chamber was filled with neuron medium containing 1% methylcellulose. Vero cells were seeded into the N chamber in a 1:1 mixture of neuron medium:Vero medium at a density that produces a confluent monolayer. Culture medium in the S chamber was replaced by 50 μl of viral inoculum containing 1×10^5 PFU in neuron medium. After 1 h at 37°C, the inoculum was removed. At 24 or 48 h postinfection (hpi), the cells in the N and S chambers were scraped and the contents of each chamber stored at −80°C.

Western blotting and immunoprecipitation. Vero cell extracts were prepared once the cytopathic effect reached 100%. Cells were treated with 1% Triton X-100, nuclei pelleted, and supernatants stored at −80°C. For immunoprecipitations, cell extracts were incubated with Fd69 anti-gI MAb and then with protein-G agarose beads (Invitrogen). Cell extracts and immunoprecipitates were separated by SDS-PAGE on 4 to 15% Tris-HCl gels (Bio-Rad) and then transferred to Immobilon P membranes and probed with the indicated antibodies. Blots were incubated with ECL substrate (GE Healthcare) and imaged on X-Omat film (Kodak).

Mouse flank infections. One day prior to infection, the right flanks of 7- to 8-week-old BALB/c mice (National Cancer Institute) were shaved and then depilated with Nair. A total of 5×10^5 PFU of HSV-1 in 10 μl was placed on the skin, and 80 gentle scratches were made through the droplet using a 27-gauge needle (8, 36). Mice were observed for disease from 3 to 11 days postinfection (dpi) and for survival until 15 dpi. Zosteriform disease was scored on a scale of 0 to 4 as follows: no lesions, 0; discrete lesions, 1; coalesced lesions, 2; ulcerated lesions, 3; and necrosis, 4. Mice that died prior to the end of observation continued to receive their last disease score. At 5 dpi, DRG from the right side of the mouse were harvested and their titer was determined. At 6 dpi, the titers of equal areas of dermatome skin at least 5 mm away from the inoculation site were determined (8). For immunohistochemistry, spinal cords were harvested 3 or 5 dpi, while zosteriform skin was harvested 5 dpi.

Mouse retina infections. For retinal infection, 8- to 9-week-old BALB/c mice were used. The temporal sclera was cut with spring scissors, and a hole was made into the vitreous body using a 27-gauge needle (51). One microliter of inoculum containing 4×10^4 to 4×10^6 PFU was injected into the vitreous body using a Hamilton syringe, and it was held in place for 30 s to prevent backflow. Mice were sacrificed 3, 5, or 8 dpi, and eyes and brains were harvested as described previously (51). Briefly, fixed tissues were sectioned on a cryostat. Eyes were cut in 10-μm sections in the saggital plane and mounted directly on slides. Brains and spinal cords were cut in 40-μm sections in the coronal plane (brains) or transverse plane (spinal cords) and transferred to cryoprotectant solution (30% sucrose, 30% ethylene glycol, 1% polyvinylpyrrolidone in PBS). Tissues were stored at −20°C until staining.

Immunofluorescence. Eye sections mounted on slides were heated at 45°C for 30 min prior to staining. Sections were incubated with rabbit anti-HSV-1 and rat anti-Thy1.2, followed by Alexa-555 anti-rabbit and Alexa-488 anti-rat secondary antibodies. Nuclei were stained with 4′,6′-diamidino-2-phenylindole (DAPI) (Invitrogen). Slides were mounted with Pro-Long Gold Antifade reagent (Invitrogen) and viewed under a Nikon Eclipse E1000 microscope with a BW Evolution QE camera.

Immunohistochemistry. Skin from zosteriform lesions was fixed in 4% formaldehyde, embedded in paraffin, stained with anti-HSV-1, and counterstained with hematoxylin (performed by the pathology core facility at the Children's Hospital of Philadelphia). Brain and spinal cord sections were stained by avidin-biotin complex immunohistochemistry as described previously (51). Sections were counterstained with cresyl violet and viewed under a Nikon Eclipse E1000 microscope with a Color Insight QE camera. Images were processed using Phase 3 imaging software and Adobe Photoshop.

Statistical analysis. All statistical analyses were performed with GraphPad Prism software.

RESULTS

Characterization of NS-Us9null. Several mutant viruses were used to assess the roles of gE, gI, and Us9 in HSV-1 neuronal spread. We performed single-step growth curves to compare the replication of NS-Us9null to that of NS in Vero cells (Fig. 2A) and in dissociated SCG neurons (Fig. 2B), and we found

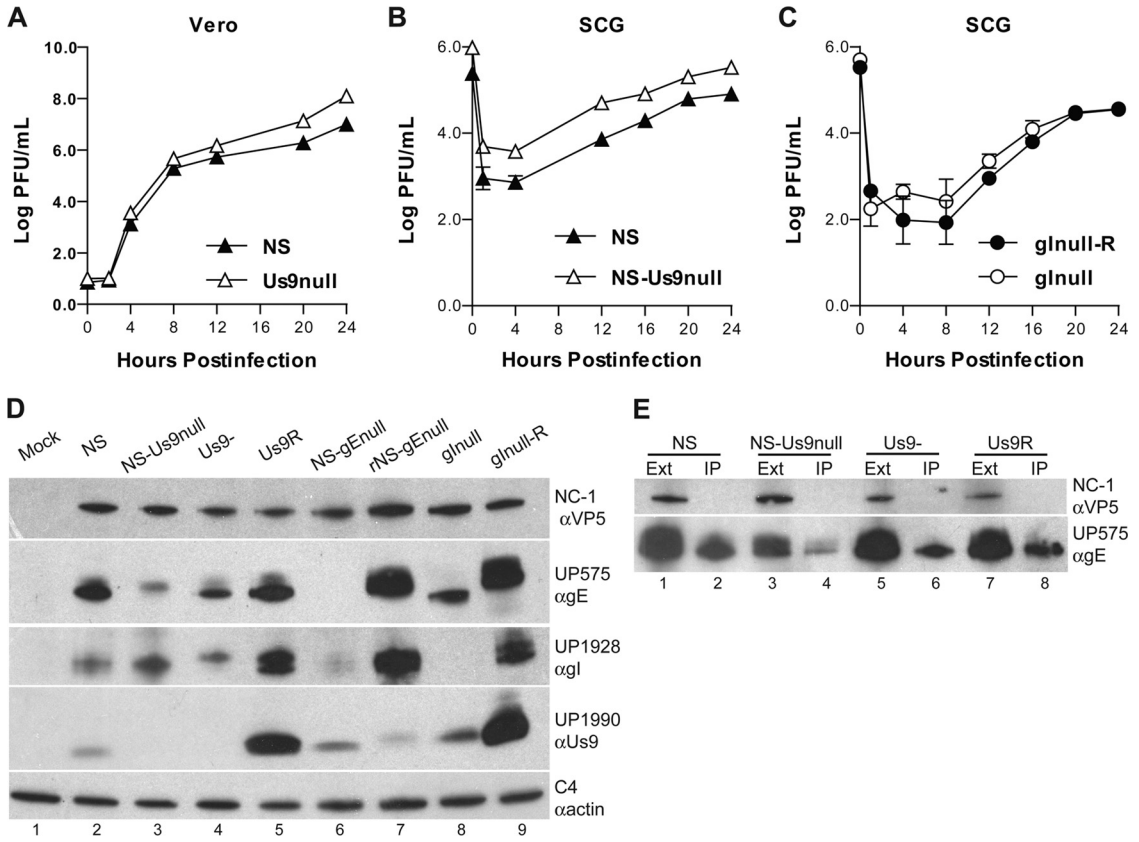

FIG. 2. Characterization of mutant viruses. (A) Vero cells were infected with HSV-1 NS or NS-Us9null at an MOI of 5. The titers of cells and media were determined together on Vero cells. Results from one experiment are shown. (B) Dissociated SCG neurons were infected with 2.5×10^5 PFU HSV-1 NS or NS-Us9null. Results shown are the means ± standard errors of two experiments. (C) Dissociated SCG neurons were infected with 2.5×10^5 PFU HSV-1 gInull-R or gInull. Results shown are the means ± standard errors of four experiments. (D) Vero cells were infected with HSV-1, and extracts were separated by SDS-PAGE and then probed by Western blotting with antibodies against VP5 (αVP5), gE (αgE), gI (αgI), Us9 (αUs9), or actin (αactin). (E) Extracts from Vero cells infected with NS, NS-Us9null, Us9-, or Us9R were immunoprecipitated with anti-gI MAb Fd69. The extracts (Ext) and immunoprecipitates (IP) were probed by Western blotting with the indicated antibodies.

that Us9 was dispensable for HSV-1 replication in vitro, consistent with reports of other Us9-deleted viruses (26, 41, 46). We found that gI also was dispensable for replication in SCG neurons (Fig. 2C), consistent with the growth curves of gInull virus in epithelial cells (3). We previously have shown that gE is dispensable for replication in SCG neurons and in epithelial cells (33).

To further characterize the mutant viruses to be used in this study, we probed infected cell lysates by Western blotting to detect gE, gI, and Us9. As expected, the previously described gE-deleted (NS-gEnull) and gI-deleted (gInull) viruses failed to express gE and gI, respectively, while the corresponding rescue viruses restored expression (Fig. 2D). Notably, NS-gEnull expresses very little gI protein compared to the rescue virus (lanes 6 and 7), while gInull expresses less gE protein than its rescue virus and only a smaller, possibly unprocessed, band (lanes 8 and 9). Two Us9-deleted viruses were used in these studies: NS-Us9null, described in this report, and Us9-, which was described previously (26). Neither Us9-deleted virus expresses Us9 protein as assessed using a polyclonal rabbit serum against Us9 (lanes 3 and 4). To confirm that gE and gI are able to form a complex in the absence of Us9, infected cell extracts were immunoprecipitated with anti-gI MAb Fd69. gE coprecipitated with gI in all samples (Fig. 2E, lanes 2, 4, 6, and 8), indicating that the gE/gI complex forms in the absence of Us9.

Anterograde spread in Campenot chambers. We used rat SCG neurons in Campenot chambers to characterize the roles of gE, gI, and Us9 in anterograde spread from neurons to epithelial cells. A total of 1×10^5 PFU of HSV-1 was added to the S chamber, and the titers of the contents of the S and N chambers were determined at 24 and 48 hpi. Although each S chamber contains approximately 5,000 SCG neurons, the neurons are sparsely distributed, and much of the inoculum adheres to the dish surface, making direct MOI calculations difficult (13, 45). In our experience, 1×10^5 PFU is at least 10 times greater than the amount of virus required to infect all neurons in the culture, as assessed by immunofluorescence staining for viral antigens. One day prior to infection, epithelial detector cells (Vero cells) were seeded into the N chamber since, as previously reported for PRV, no virus was detected in the N chamber in the absence of epithelial cells (data not shown) (13). S chamber titers remained approximately constant from 24 to 48 hpi, which was expected, since sufficient virus was added to infect all neurons in the S chamber. Overall, S chamber titers at 24 and 48 hpi were similar for the mutant

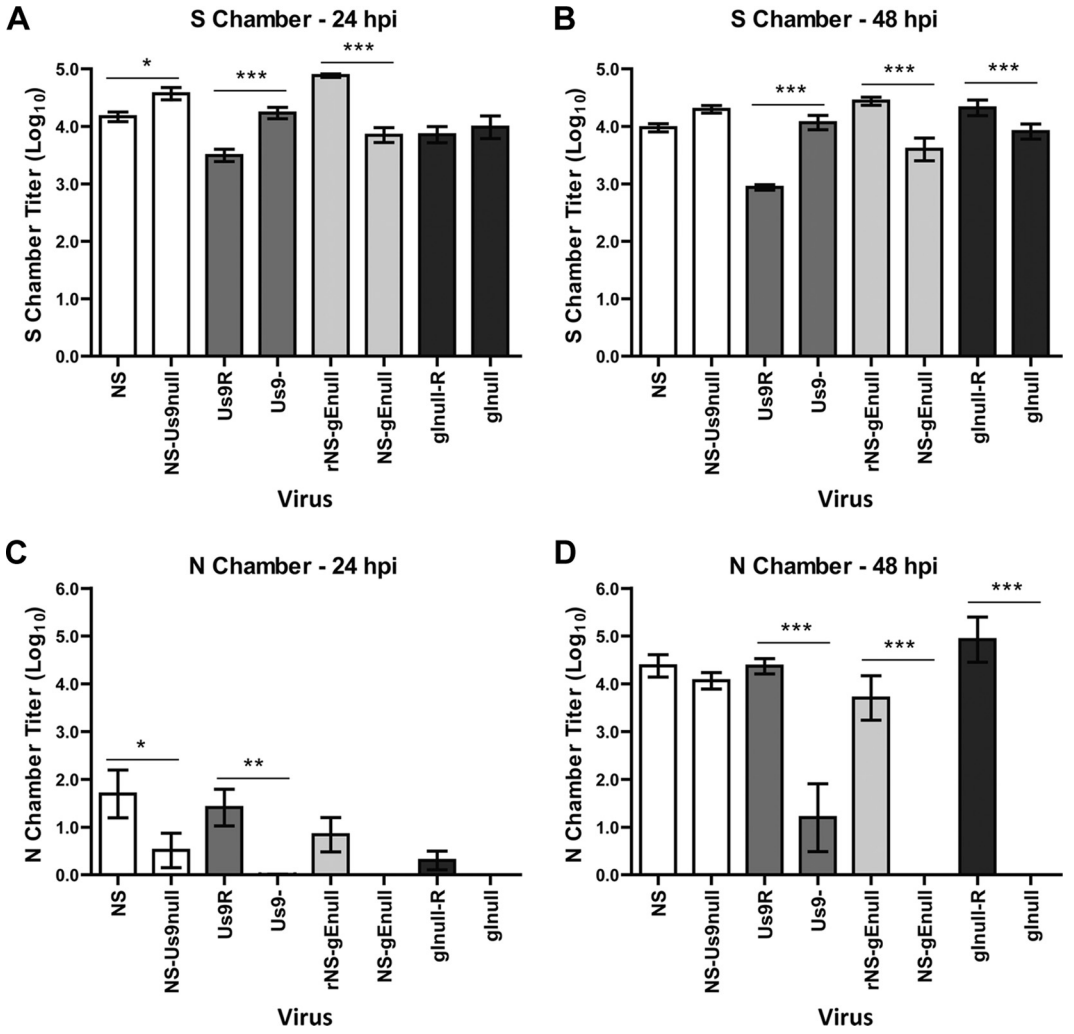

FIG. 3. Anterograde spread in Campenot chambers. A total of 1×10^5 PFU WT, mutant, or rescue strain HSV-1 was added to the S chamber. The titers of the contents of the S (A and B) and N (C and D) chambers were determined on Vero cells 24 (A and C) or 48 (B and D) hpi. Results shown are means ± standard errors of six chambers per virus strain at each time point. *, $P < 0.05$; **, $P < 0.01$; ***, $P < 0.001$.

and parental or rescue strains, although some variability occurred (Fig. 3A and B).

At 48 hpi, titers of all mutant viruses were approximately 4 $\log_{10}$ in the S chamber, yet large differences in titers were apparent in the N chamber (Fig. 3B and D). N chamber titers of all viruses were low at 24 hpi (Fig. 3C); however, even at 48 hpi, no NS-gEnull or gInull virus was detected in the N chamber, whereas the rescue virus had titers of 4 to 5 $\log_{10}$. This result is consistent with the previous finding that NS-gEnull has a complete anterograde spread defect in the mouse retina model of infection (51). Surprisingly, both Us9-deleted viruses retained anterograde spread activity in the Campenot chamber system (Fig. 3D). There was no significant difference between the N chamber titers of NS and NS-Us9null at 48 hpi, indicating that this virus retains anterograde spread activity. N chamber titers of Us9- were significantly lower than those of Us9R (approximately 3 $\log_{10}$ reduced), but some anterograde spread was detected. These results suggest that Us9- has a partial defect in anterograde spread, but that this defect is much less severe than the complete anterograde spread defects of the gEnull and gInull viruses. Virus detected in the N chamber after NS-Us9null and Us9- infection was confirmed by Western blotting not to express Us9 protein.

Mouse retina infection model. We used the mouse retina infection model (Fig. 1B) to further define the anterograde spread properties of the Us9 mutant viruses and to characterize gInull and gInull-R in this system. The phenotype of NS-gEnull in the mouse retina model has been published previously (51). Mice were injected with 4×10^4 PFU HSV-1 NS, NS-Us9null, Us9-, Us9R, or gInull-R, while 4×10^5 PFU of gInull virus was inoculated.

Anterograde axonal transport into the optic nerve. At 5 dpi, all six viruses tested showed extensive infection of the retina, as assessed by immunofluorescence with an anti-HSV-1 antibody (Fig. 4A). Viral antigens were detected in the optic nerve after infection with NS-Us9null and Us9-, indicating the anterograde axonal transport of viral proteins. This antigen staining was indistinguishable from NS and Us9R staining. Similar optic nerve staining was observed for NS and NS-Us9null at 3 dpi (data not shown). In contrast, no viral antigen was detected in

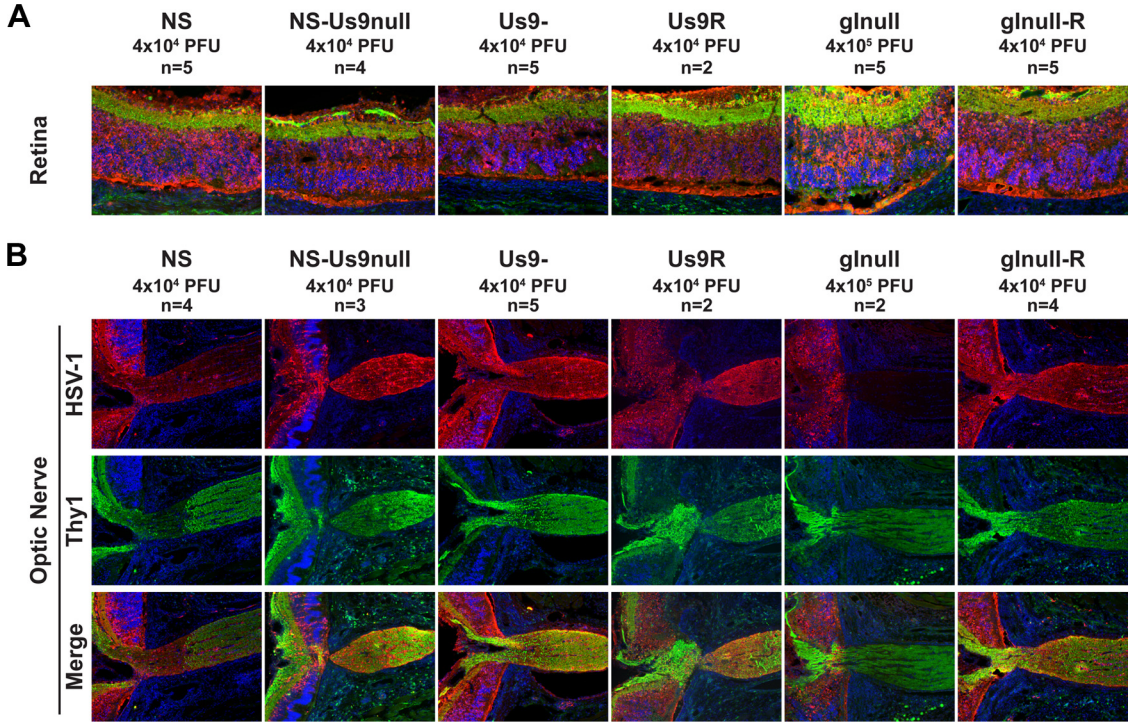

FIG. 4. Anterograde transport into the optic nerve. Mice were infected in the vitreous body with WT, mutant, or rescue strain HSV-1, and tissues were harvested 5 dpi. Sections were stained for immunofluorescence with anti-HSV-1 (red), the neuronal marker anti-Thy1 (green), and DAPI (blue). (A) Ganglion cell neurons form the innermost layer of the retina, which is shown in green at the top of each image. Magnification, ×200. (B) The retina is shown on the left side of each image, while the optic nerve is shown on the right, at the site of exit from the retina. Magnification, ×100.

the optic nerve after gInull virus infection, despite extensive infection of the retina (Fig. 4A) and infection with titers 10 times greater than that of gInull-R. This phenotype is identical to that of NS-gEnull in the mouse retina model and is consistent with the Campenot chamber results (51).

Anterograde and retrograde spread to the brain. At 5 dpi, WT and rescue viruses showed extensive spread to the brain along visual pathways (anterograde spread) as well as along parasympathetic and motor pathways (retrograde spread) (Fig. 5). After gInull virus infection, no viral antigen was detected along visual pathways at 5 dpi (Fig. 5), as expected from the absence of viral antigen in the optic nerve. Even when the input dose was increased to 4×10^6 PFU and tissue was harvested 8 dpi, no antigen was detected along visual pathways (data not shown). This observation, along with the Campenot chamber data, suggests that gI is essential for anterograde axonal transport, and thus the anterograde spread, of HSV-1. Interestingly, viral antigen was detected in nuclei reached by retrograde spread after gInull infection (Fig. 5A and C), although the extent of staining was greatly reduced compared to that of the rescue virus.

Both NS-Us9null and Us9- showed extensive antigen staining in nuclei reached by retrograde spread (Fig. 5A and C), confirming previous reports that Us9 is dispensable for HSV-1 retrograde spread (26, 41). The optic tract is the extension of the optic nerve into the brain, and consistent with the staining observed in the optic nerve (Fig. 4B), viral antigen was detected in the optic tract after NS-Us9null and Us9- infection (Fig. 5A and B). Viral antigen also was detected at second-order sites along the visual pathway, including the lateral geniculate nucleus (Fig. 5B) and superior colliculus (Fig. 5C), although the amount of staining at these sites was greatly reduced compared to that with NS and Us9R. Spread to these second-order sites requires the virus to cross a synapse, indicating that all of the components necessary to produce infectious virus were transported into the optic nerve and optic tract.

To verify that all classes of viral proteins are transported into optic nerve axons in the absence of Us9, brains were stained 5 dpi with antibodies specific to viral glycoproteins, tegument, or capsid (Fig. 6). In BALB/c mice, nearly all optic nerve axons cross the midline, so viral antigens in the optic tract are detected mainly on the side contralateral to the injected eye. The general lack of staining in the ipsilateral optic tract confirms the specificity of the antibody staining, although bilateral optic tract staining sometimes is observed. Glycoprotein (Fig. 6A), tegument (Fig. 6B), and capsid (Fig. 6C) antigens were detected in the optic tracts of mice infected with NS, NS-Us9null, Us9-, or Us9R, indicating that Us9 is not required for the anterograde transport of these proteins. Antigen staining in the ipsilateral optic tract was somewhat reduced for NS-Us9null and Us9- compared to that of NS and Us9R, which suggests that the mutant viruses are slightly impaired at anterograde transport. At 3 dpi, NS-Us9null and Us9- showed staining patterns identical to that of NS, although all three

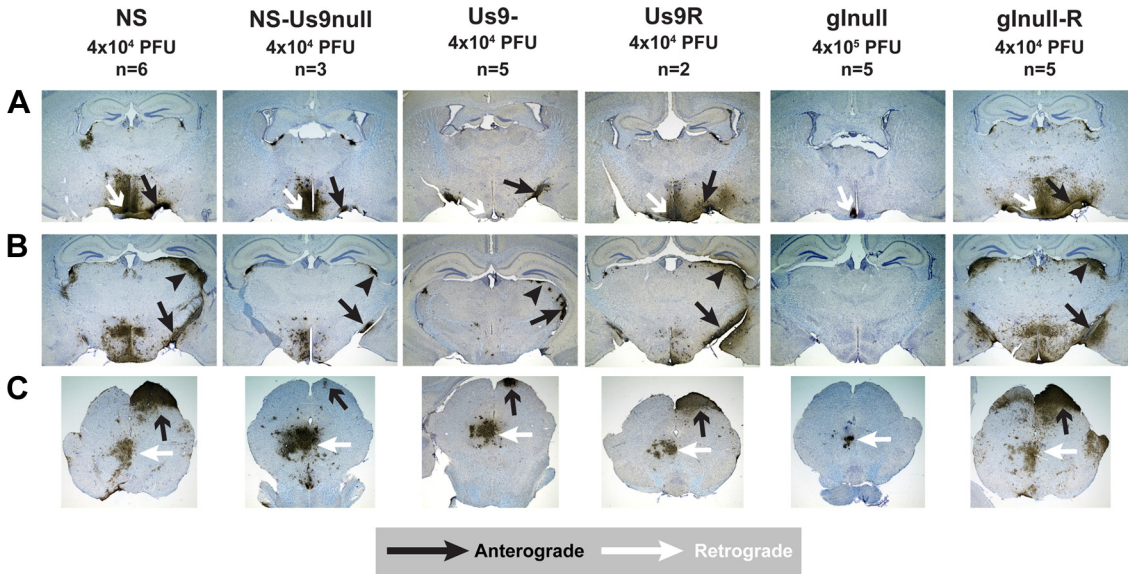

FIG. 5. Spread to the brain. Mice were infected in the vitreous body with WT, mutant, or rescue strain HSV-1, and tissues were harvested 5 dpi. (A) Anterograde transport to the optic tract (black arrows) and multisynaptic retrograde spread to the suprachiasmatic nucleus (white arrows). (B) Anterograde transport to the optic tract (black arrows) and anterograde spread to the lateral geniculate nucleus (black arrowheads). (C) Anterograde spread to the superior colliculus (black arrows) and retrograde spread to the oculomotor and Edinger-Westphal nuclei (white arrows). Magnification, ×20.

viruses had only minimal antigen in the brain at this early time point (data not shown).

Zosteriform disease in the mouse flank model. To further analyze the spread properties of the two Us9-deleted viruses, we employed the mouse flank model (Fig. 1A) (8, 36). Several types of spread are required to produce zosteriform lesions, including (i) cell-to-cell spread between epithelial cells at the inoculation site; (ii) epithelial-to-neurite spread; (iii) retrograde axonal transport; (iv) spread to multiple neurons within the DRG; (v) anterograde axonal transport; and (vi) neurite-to-epithelial spread at the zosteriform site. Thus, the production of zosteriform disease represents a rigorous test of viral spread.

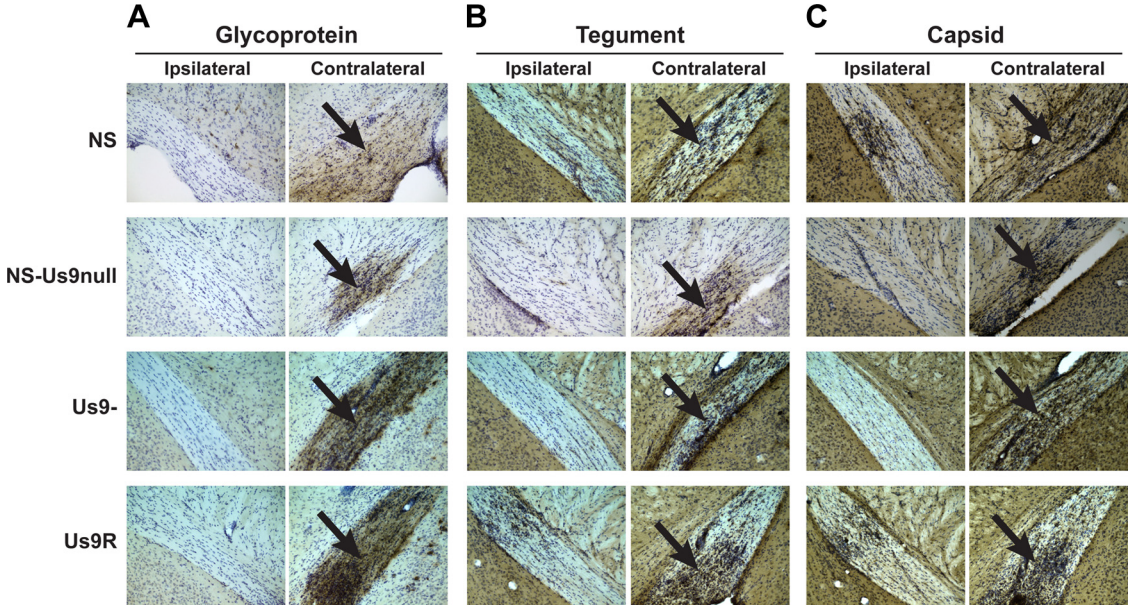

FIG. 6. Glycoprotein, tegument, and capsid antigens are transported into the optic tract. Mice were infected in the vitreous body with 4×10^4 PFU HSV-1 NS, NS-Us9null, Us9-, or Us9R, and tissues were harvested 5 dpi. Optic tracts ipsilateral and contralateral to the injected eye are shown at ×200 magnification. Antigen staining in the contralateral optic tract is indicated with black arrows. Brains were stained with the following antibodies against glycoprotein, tegument, or capsid: R122 anti-gD (NS, NS-Us9null) or R118 anti-gC (Us9-, Us9R) (A); PSU74 anti-VP22 (B); and NC-L anti-capsid (C). The antibodies against VP22 and light capsid produced higher background staining levels than did the antibodies against gD and gC.

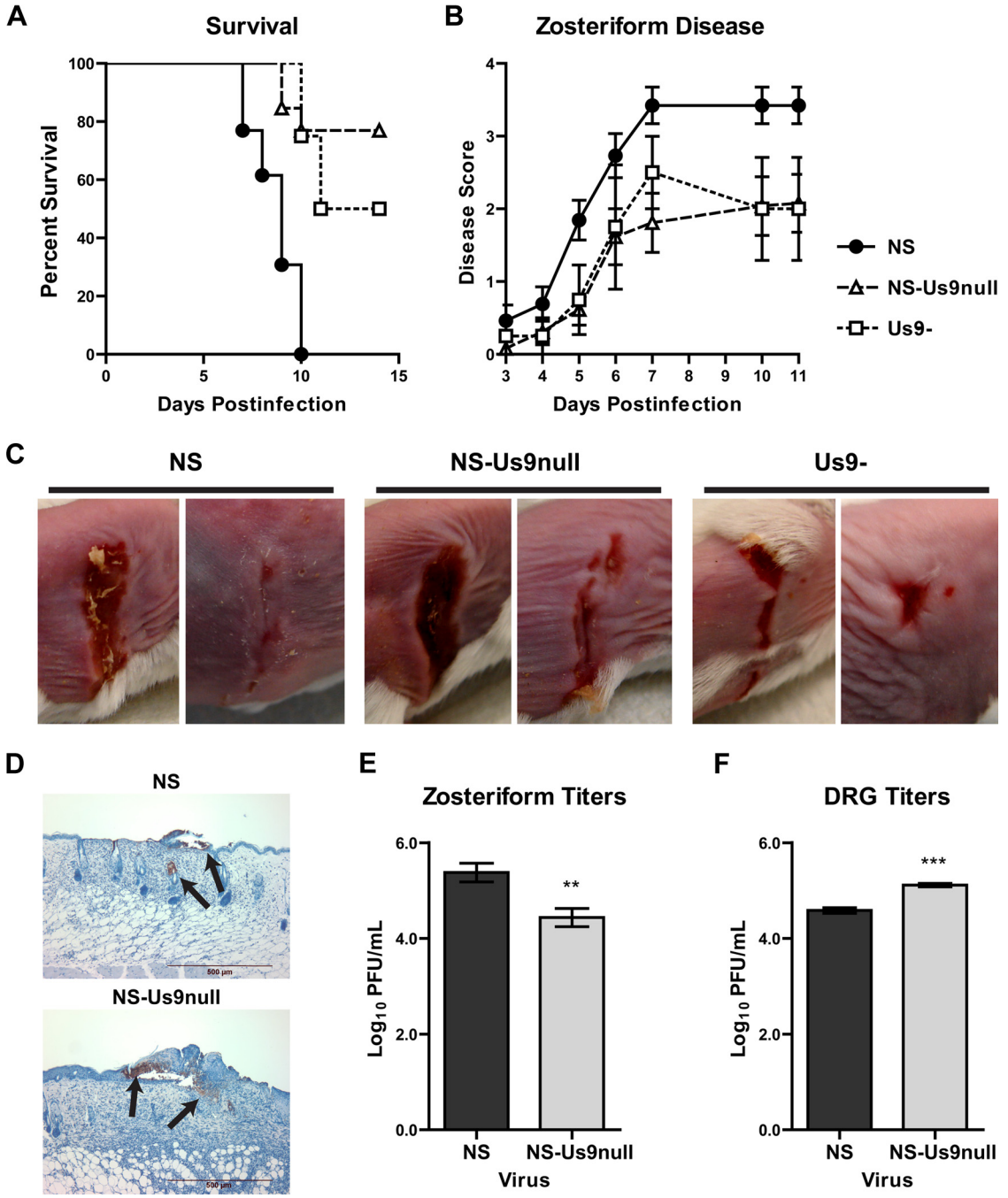

FIG. 7. Zosteriform disease in the mouse flank model. Mice were scratch inoculated with 5×10^5 PFU NS, NS-Us9null, or Us9-. (A) The percentage of mice surviving was recorded for 15 dpi. For comparisons of NS to NS-Us9null or Us9-, $P < 0.01$; for comparisons of Us9- to NS-Us9null, $P > 0.05$. (B) The severity of zosteriform disease was measured 3 to 11 dpi. For comparisons of NS to NS-Us9null or Us9-, $P < 0.001$; for comparisons of Us9- to NS-Us9null, $P > 0.05$. For NS and NS-Us9null, $n = 13$; for Us9-, $n = 4$. (C) Zosteriform disease was photographed 7 dpi. (D) Zosteriform lesions from NS- or NS-Us9null-infected mice were stained with anti-HSV-1 and counterstained with hematoxylin. Viral antigen staining is indicated by the arrows. (E) Viral titers in zosteriform lesions 6 dpi. **, $P < 0.01$ ($n = 9$). (F) Viral titers in DRG 5 dpi. ***, $P < 0.001$ ($n = 5$).

Mice were scratch inoculated with 5×10^5 PFU NS, NS-Us9null, or Us9- and monitored for survival and zosteriform disease. Both Us9-deleted viruses were significantly less lethal than NS, but they were not significantly different from each other. No mouse infected with NS survived past day 10, while 80 and 50% of mice infected with NS-Us9null and Us9-, respectively, survived past day 15 (Fig. 7A). Zosteriform lesions were observed in 13 of 13 mice infected with NS, 10 of 13 mice infected with NS-Us9null, and 4 of 4 mice infected with Us9-. NS-Us9null and Us9- disease scores were significantly lower

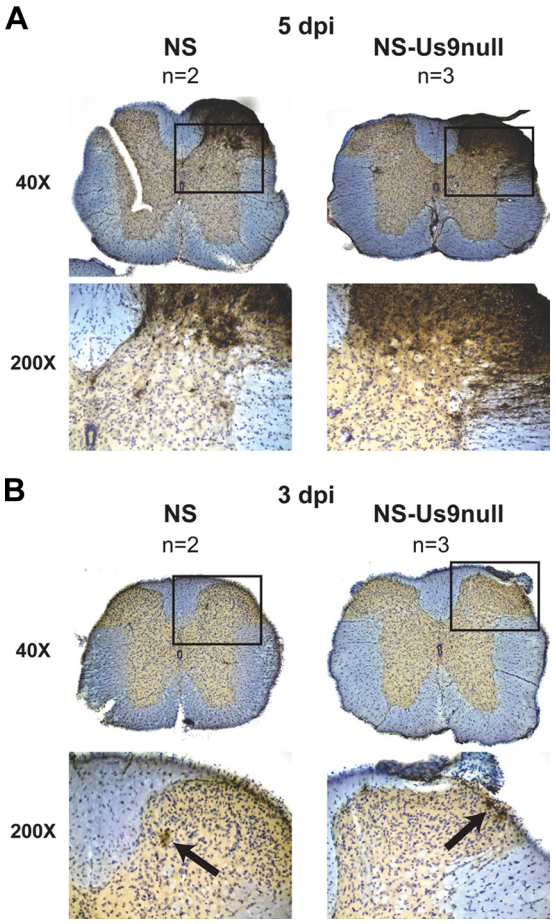

FIG. 8. Viral spread to the spinal cord. Mice were flank inoculated with 4×10^5 PFU NS or NS-Us9null. Spinal cords were dissected 5 (A) or 3 (B) dpi. Sections were stained with anti-HSV-1 and counterstained with cresyl violet. The boxed areas at ×40 magnification are shown at ×200 magnification below. Black arrows indicate viral antigen staining at 3 dpi.

than those of NS (Fig. 7B), although some mice infected with each virus developed substantial zosteriform disease (Fig. 7C). The presence of viral antigen in NS and NS-Us9null zosteriform lesions was confirmed by immunohistochemistry (Fig. 7D). Viral titers from NS-Us9null zosteriform lesions were lower than those of NS, consistent with the disease scores for each virus (Fig. 7E). NS-Us9null produced higher titers than NS in DRG, indicating that reduced zosteriform disease was not a consequence of impaired spread to the DRG (Fig. 7F).

Anterograde spread to the spinal cord. Once HSV-1 reaches the DRG after flank inoculation, it can return to the skin in an anterograde direction to produce zosteriform disease. However, since DRG sensory neurons are pseudounipolar, HSV-1 also can spread in the anterograde direction from the DRG to the dorsal horn of the spinal cord and then spread transynaptically to other spinal cord neurons (Fig. 1A). At 5 dpi, extensive viral antigen was detected in the dorsal horn of the spinal cord after NS or NS-Us9null infection, indicating intact anterograde transport and transynaptic anterograde spread (Fig. 8A). Occasional ventral horn staining was observed, suggesting retrograde spread via motor neurons, but the most abundant staining was in the dorsal horn. Staining of nuclei across the midline also was observed, indicating multisynaptic spread. At 3 dpi (Fig. 8B), very little antigen was detected in the spinal cord, but all staining at that time was in the dorsal horn. At both 5 and 3 dpi, the staining pattern after NS-Us9null infection was indistinguishable from that of NS. The presence of viral antigen in the dorsal horn of the spinal cord and the production of zosteriform lesions after flank inoculation with NS-Us9null indicate that Us9 is dispensable for anterograde neuronal spread.

DISCUSSION

Previous work has implicated three viral proteins, gE, gI, and Us9, in the anterograde axonal transport or anterograde neuronal spread of the alphaherpesviruses HSV-1, PRV, BHV-1, and BHV-5 (2, 5, 7, 9, 11, 13, 16, 26, 29–31, 41, 46, 51, 52). Here, we show that gE and gI are essential for HSV-1 anterograde spread, while Us9 plays a nonessential contributing role (Table 1). We confirmed the Us9 phenotype using two independent Us9-deleted viruses from two different strains of HSV-1. We characterized the anterograde spread properties of the two viruses in three different model systems, some of which had multiple readouts for anterograde spread. We also showed that, like gE, HSV-1 gI is required for anterograde axonal transport in the mouse retina model; however, unlike NS-gEnull, gInull retained some retrograde spread activity.

In Campenot chamber experiments to assess HSV-1 anterograde spread, virus was detected in the N chamber only in the presence of Vero cells; no virus was detected from neurites alone. Similarly, any of several epithelial cell types permit PRV detection in the N chamber, but no virus is detected from free neurites (13). In contrast, West Nile virus can be detected from free N chamber neurites, although the titers are much lower without amplification in epithelial cells (43). This observation indicates that SCG neurons are not generally defective at virus release and that the requirement for epithelial cells may be specific to the molecular mechanisms used by alphaherpesviruses for axonal egress.

Like HSV-1 gEnull and gInull, PRV gEnull, gInull, and Us9null viruses have complete anterograde spread defects in animal models (2, 5, 7, 11, 29, 52). However, the Campenot chamber system revealed that these PRV mutants retain partial anterograde spread activity in vitro (13). In contrast, we

TABLE 1. Anterograde transport and spread phenotypes of gE-, gI-, and Us9-deleted viruses in three model systems[a]

Virus	Campenot	Retina		Flank	
		Optic Tract	LGN/SC	Zosteriform	Dorsal Horn
NS	+++	+++	+++	+++	+++
NS-Us9null	+++	+++	+	++	+++
Us9-	+	+++	+	++	ND
NS-gEnull	−	− (51)	− (51)	# (8, 36)	ND
gInull	−	−	−	ND	ND

[a] Phenotypes are graded on the following scale: no spread (−), some spread (+), moderate spread (++), extensive spread (+++). ND, no data; LGN, lateral geniculate nucleus; SC, superior colliculus; #, NS-gEnull fails to reach the DRG, so zosteriform disease cannot be evaluated. Numbers in parentheses indicate references that report the results shown.

detected no HSV-1 gEnull or gInull virus in the N chamber at 48 hpi, when WT and rescued viruses had achieved titers of 4 to 5 $\log_{10}$. These results suggest that gE and gI play a role in HSV-1 anterograde axonal transport or spread that is more pronounced than that for PRV.

The absence of antigen in the optic nerve after NS-gEnull and gInull infection suggests that viral proteins are unable to traffic into the axon in the absence of gE or gI. This result is consistent with observations with differentiated neuroblastoma cells, in which the axonal localization of capsid and glycoproteins was reduced in the absence of gE and gI (46). This reduced axonal localization was particularly pronounced at more distal regions of the axon (20 to 25 μm). Since retinal ganglion cell bodies may be 1 mm or more from their axons in the optic nerve, anterograde transport defects should be clearly evident in the optic nerve. Although in the absence of gE or gI we failed to detect any viral antigens in the optic nerve using a polyclonal anti-HSV-1 antibody, we cannot exclude that certain viral proteins not detected by this antibody were able to traffic into the optic nerve (51).

Conclusions about the individual importance of gE and gI in HSV-1 spread are confounded by the fact that NS-gEnull and gInull have reduced expression of gI and gE, respectively. Thus, the phenotype of each deletion virus could be caused by reduced levels of the other protein. gE and gI have been reported to have variable effects on one another's processing in many alphaherpesviruses, although the implications of this for spread and virulence are unclear (1, 6, 20, 35, 37, 48, 52, 53).

Direct comparisons between the gEnull and gInull viruses in this study are further complicated by the fact that these two mutants are in different strains of HSV-1 (NS and SC16, respectively). Since some retrograde spread to the brain was detected in gInull-infected animals, while NS-gEnull is completely defective at retrograde spread, it is tempting to postulate that gE is more critical for retrograde spread than gI (51). However, it is possible that SC16 is more neuroinvasive than NS, explaining the residual retrograde spread activity of the gInull virus. A strain SC16 gEnull virus retained some retrograde spread in the mouse pinna infection model, but at reduced levels compared to those of gInull (3). Additional isogenic gEnull and gInull mutants are needed to further compare the relative roles of gE and gI in HSV-1 retrograde spread.

Interestingly, PRV Us9null virus has a stronger anterograde spread defect than PRV gEnull or gInull virus (13, 29–32). In contrast, here we showed that two independent HSV-1 Us9-deleted viruses have only minimal anterograde spread defects compared to the complete defects of HSV-1 gEnull and gInull viruses. In fact, since both Us9-deleted viruses have reduced gE and/or gI expression, it may be that the lack of sufficient gE or gI contributes to the minor anterograde spread defects of these viruses. It seems that the relative contributions of gE/gI and Us9 to the anterograde spread of HSV-1 and PRV are reversed, such that gE and gI are the main effectors in HSV-1 while Us9 is the main effector in PRV. Consistent with this possibility, the Us9 genes of equine herpes virus and of BHV-1 are able to complement the anterograde spread defect of a PRV Us9null virus, whereas VZV and HSV-1 Us9 do not complement the PRV mutant (32). These observations support the conclusion that HSV-1 Us9 plays a different role in anterograde spread than does PRV Us9.

We used three different experimental systems to rigorously characterize the anterograde spread properties of the Us9-deleted viruses (Table 1). In the Campenot chamber system, NS-Us9null retained complete anterograde spread activity, while Us9- N chamber titers were reduced. In the mouse retina model, both Us9 mutant viruses showed equivalent anterograde axonal transport (optic nerve and optic tract), although transneuronal spread along visual pathways (to the lateral geniculate nucleus and superior colliculus) was greatly reduced compared to those of the WT and rescue viruses. In the mouse flank model, NS-Us9null and Us9- both produced substantial zosteriform disease, although it was less severe than NS disease. After flank inoculation, the anterograde spread of NS-Us9null into the spinal cord was indistinguishable from that of NS. Therefore, Campenot chambers were the only system in which the phenotypes of the two Us9-deleted viruses differed from each other. The Campenot system is more quantitative than animal models and may reveal subtle transport phenotypes that are not evident in vivo. The slight differences in spread phenotypes observed in the various model systems also may reflect the particular cell types that the virus spreads through in each system, e.g., epithelial-to-neuron or neuron-to-neuron spread.

Our results differ from the phenotypes of Us9null viruses reported by others (26, 41, 46). Although the reasons for the conflicting observations are unclear, there are several possible explanations. First, variability in experimental systems may produce differing conclusions. We note here that different spread phenotypes were observed in the model systems we used. Two distinct HSV-1 Us9-deleted viruses (both derived from strain F) have been studied in mouse retina models similar to the one used in this report. In both cases, the authors concluded that the Us9null virus failed to spread in an anterograde direction to visual centers in the brain (26, 41). However, Polcicova et al. note that 80% of mice infected with their Us9null virus had no antigen at all in the brain, while 20% had limited antigen in the suprachiasmatic nucleus only (41). This observation is surprising, since the Us9null virus would be expected to retain retrograde spread activity, meaning that extensive antigen staining would be detected in the Edinger-Westphal and oculomotor nuclei, in addition to the suprachiasmatic nucleus. That this was not the case suggests that the infections were inefficient, or that this virus has additional spread defects independent of Us9.

Using a different murine model, Polcicova et al. detected greatly reduced anterograde spread of their Us9null virus from the trigeminal ganglia to the cornea: virus was recovered from only 29% of Us9null-infected mice, compared to 81% infected with the rescue virus (41). They reported that corneal titers of the Us9null virus were reduced 2 $\log_{10}$ compared to those of the rescue virus. We observed a similar reduction in titers for Us9- virus in the Campenot system; however, based on all of the models evaluated, we concluded that Us9 contributes to, but is not essential for, anterograde spread. LaVail et al. noted that the amount of viral genome detected in the optic nerve after Us9- infection was 7% of WT levels (i.e., slightly more than 1 $\log_{10}$ reduced), indicating an anterograde spread defect for this virus (26). These findings support a nonessential, al-

though contributing, role for Us9. These investigators failed to detect capsid antigens in the optic tract of mice infected with Us9-, which differs from our results. However, LaVail et al. administered valacyclovir at 24 hpi, which would reduce the amount of viral antigens produced.

Snyder et al. used immunofluorescence to detect viral proteins in the axons of differentiated neuroblastoma cells (46). They reported that cells infected with a Us9-deleted virus had fewer glycoprotein- and capsid-positive puncta in their axons than the rescue virus, suggesting similar anterograde transport defects for gEnull, gInull, and Us9null viruses. In contrast, we found that viral antigen staining in the optic nerve and optic tract (the axons of retinal neurons) was identical for NS, NS-Us9null, Us9-, and Us9R, and we detected all classes of structural proteins in the optic tract. We found that the Us9-deleted viruses have a different phenotype than the gEnull and gInull viruses, suggesting that gE and gI are the main effectors of HSV-1 anterograde spread.

Other studies of the role of Us9 in HSV-1 anterograde spread have concluded that Us9 is an important mediator of this process, but in all cases some residual anterograde spread was observed for the mutant virus. Thus, those findings may differ only in degree from the observations reported here. However, the important conclusion from our results is that the contribution of Us9 to anterograde transport within neurons or anterograde spread between axons and epithelial cells is minor compared to the roles of gE and gI.

ACKNOWLEDGMENTS

This work was supported by NIH grant AI33063.

We thank M. G. Lyman and L. W. Enquist for providing NS-Us9null; J. H. LaVail for Us9- and the rescue strain; T. Minson for gInull and rescue viruses; G. H. Cohen and R. J. Eisenberg for NC-1, NC-L, R118, and R122 sera; B. Roizman for anti-Us9 serum; and R. Courtney for anti-VP22 serum.

REFERENCES

1. **Al-Mubarak, A., and S. I. Chowdhury.** 2004. In the absence of glycoprotein I (gI), gE determines bovine herpesvirus type 5 neuroinvasiveness and neurovirulence. J. Neurovirol. **10:**233–243.
2. **Babic, N., B. Klupp, A. Brack, T. C. Mettenleiter, G. Ugolini, and A. Flamand.** 1996. Deletion of glycoprotein gE reduces the propagation of pseudorabies virus in the nervous system of mice after intranasal inoculation. Virology **219:**279–284.
3. **Balan, P., N. Davis-Poynter, S. Bell, H. Atkinson, H. Browne, and T. Minson.** 1994. An analysis of the in vitro and in vivo phenotypes of mutants of herpes simplex virus type 1 lacking glycoproteins gG, gE, gI or the putative gJ. J. Gen. Virol. **75:**1245–1258.
4. **Brideau, A. D., B. W. Banfield, and L. W. Enquist.** 1998. The Us9 gene product of pseudorabies virus, an alphaherpesvirus, is a phosphorylated, tail-anchored type II membrane protein. J. Virol. **72:**4560–4570.
5. **Brideau, A. D., J. P. Card, and L. W. Enquist.** 2000. Role of pseudorabies virus Us9, a type II membrane protein, in infection of tissue culture cells and the rat nervous system. J. Virol. **74:**834–845.
6. **Brideau, A. D., L. W. Enquist, and R. S. Tirabassi.** 2000. The role of virion membrane protein endocytosis in the herpesvirus life cycle. J. Clin. Virol. **17:**69–82.
7. **Brittle, E. E., A. E. Reynolds, and L. W. Enquist.** 2004. Two modes of pseudorabies virus neuroinvasion and lethality in mice. J. Virol. **78:**12951–12963.
8. **Brittle, E. E., F. Wang, J. M. Lubinski, R. M. Bunte, and H. M. Friedman.** 2008. A replication-competent, neuronal spread-defective, live attenuated herpes simplex virus type 1 vaccine. J. Virol. **82:**8431–8441.
9. **Butchi, N. B., C. Jones, S. Perez, A. Doster, and S. I. Chowdhury.** 2007. Envelope protein Us9 is required for the anterograde transport of bovine herpesvirus type 1 from trigeminal ganglia to nose and eye upon reactivation. J. Neurovirol. **13:**384–388.
10. **Campenot, R. B.** 1992. Compartmented culture analysis of nerve growth, p. 275–298. *In* B. Stevenson, D. Paul, and W. Gallin (ed.), Cell-cell interactions: a practical approach. Oxford University Press, New York, NY.
11. **Card, J. P., M. E. Whealy, A. K. Robbins, and L. W. Enquist.** 1992. Pseudorabies virus envelope glycoprotein gI influences both neurotropism and virulence during infection of the rat visual system. J. Virol. **66:**3032–3041.
12. **Card, J. P., M. E. Whealy, A. K. Robbins, R. Y. Moore, and L. W. Enquist.** 1991. Two alpha-herpesvirus strains are transported differentially in the rodent visual system. Neuron **6:**957–969.
13. **Ch'ng, T. H., and L. W. Enquist.** 2005. Neuron-to-cell spread of pseudorabies virus in a compartmented neuronal culture system. J. Virol. **79:**10875–10889.
14. **Ch'ng, T. H., E. A. Flood, and L. W. Enquist.** 2005. Culturing primary and transformed neuronal cells for studying pseudorabies virus infection. Methods Mol. Biol. **292:**299–316.
15. **Chowdhury, S. I., B. J. Lee, A. Ozkul, and M. L. Weiss.** 2000. Bovine herpesvirus 5 glycoprotein E is important for neuroinvasiveness and neurovirulence in the olfactory pathway of the rabbit. J. Virol. **74:**2094–2106.
16. **Chowdhury, S. I., M. Onderci, P. S. Bhattacharjee, A. Al-Mubarak, M. L. Weiss, and Y. Zhou.** 2002. Bovine herpesvirus 5 (BHV-5) Us9 is essential for BHV-5 neuropathogenesis. J. Virol. **76:**3839–3851.
17. **Cohen, G. H., M. Ponce de Leon, H. Diggelmann, W. C. Lawrence, S. K. Vernon, and R. J. Eisenberg.** 1980. Structural analysis of the capsid polypeptides of herpes simplex virus types 1 and 2. J. Virol. **34:**521–531.
18. **Cohen, J. I., H. Sato, S. Srinivas, and K. Lekstrom.** 2001. Varicella-zoster virus (VZV) ORF65 virion protein is dispensable for replication in cell culture and is phosphorylated by casein kinase II, but not by the VZV protein kinases. Virology **280:**62–71.
19. **Diefenbach, R. J., M. Miranda-Saksena, M. W. Douglas, and A. L. Cunningham.** 2008. Transport and egress of herpes simplex virus in neurons. Rev. Med. Virol. **18:**35–51.
20. **Dingwell, K. S., C. R. Brunetti, R. L. Hendricks, Q. Tang, M. Tang, A. J. Rainbow, and D. C. Johnson.** 1994. Herpes simplex virus glycoproteins E and I facilitate cell-to-cell spread in vivo and across junctions of cultured cells. J. Virol. **68:**834–845.
21. **Dingwell, K. S., L. C. Doering, and D. C. Johnson.** 1995. Glycoproteins E and I facilitate neuron-to-neuron spread of herpes simplex virus. J. Virol. **69:**7087–7098.
22. **Enquist, L. W., P. J. Husak, B. W. Banfield, and G. A. Smith.** 1998. Infection and spread of alphaherpesviruses in the nervous system. Adv. Virus Res. **51:**237–347.
23. **Friedman, H. M., E. J. Macarak, R. R. MacGregor, J. Wolfe, and N. A. Kefalides.** 1981. Virus infection of endothelial cells. J. Infect. Dis. **143:**266–273.
24. **Hook, L. M., J. Huang, M. Jiang, R. Hodinka, and H. M. Friedman.** 2008. Blocking antibody access to neutralizing domains on glycoproteins involved in entry as a novel mechanism of immune evasion by herpes simplex virus type 1 glycoproteins C and E. J. Virol. **82:**6935–6941.
25. **Husak, P. J., T. Kuo, and L. W. Enquist.** 2000. Pseudorabies virus membrane proteins gI and gE facilitate anterograde spread of infection in projection-specific neurons in the rat. J. Virol. **74:**10975–10983.
26. **LaVail, J. H., A. N. Tauscher, A. Sucher, O. Harrabi, and R. Brandimarti.** 2007. Viral regulation of the long distance axonal transport of herpes simplex virus nucleocapsid. Neuroscience **146:**974–985.
27. **Lin, X., J. M. Lubinski, and H. M. Friedman.** 2004. Immunization strategies to block the herpes simplex virus type 1 immunoglobulin G Fc receptor. J. Virol. **78:**2562–2571.
28. **Longnecker, R., S. Chatterjee, R. J. Whitley, and B. Roizman.** 1987. Identification of a herpes simplex virus 1 glycoprotein gene within a gene cluster dispensable for growth in cell culture. Proc. Natl. Acad. Sci. USA **84:**4303–4307.
29. **Lyman, M. G., D. Curanovic, A. D. Brideau, and L. W. Enquist.** 2008. Fusion of enhanced green fluorescent protein to the pseudorabies virus axonal sorting protein Us9 blocks anterograde spread of infection in mammalian neurons. J. Virol. **82:**10308–10311.
30. **Lyman, M. G., D. Curanovic, and L. W. Enquist.** 2008. Targeting of pseudorabies virus structural proteins to axons requires association of the viral Us9 protein with lipid rafts. PLoS Pathog. **4:**e1000065.
31. **Lyman, M. G., B. Feierbach, D. Curanovic, M. Bisher, and L. W. Enquist.** 2007. Pseudorabies virus Us9 directs axonal sorting of viral capsids. J. Virol. **81:**11363–11371.
32. **Lyman, M. G., C. D. Kemp, M. P. Taylor, and L. W. Enquist.** 2009. A comparison of the pseudorabies virus Us9 protein with homologs from other veterinary and human alphaherpesviruses. J. Virol. **83:**6978–6986.
33. **McGraw, H. M., and H. M. Friedman.** 2009. Herpes simplex virus type 1 glycoprotein E mediates retrograde spread from epithelial cells to neurites. J. Virol. **83:**4791–4799.
34. **Mijnes, J. D., B. C. Lutters, A. C. Vlot, E. van Anken, M. C. Horzinek, P. J. Rottier, and R. J. de Groot.** 1997. Structure-function analysis of the gE-gI complex of feline herpesvirus: mapping of gI domains required for gE-gI interaction, intracellular transport, and cell-to-cell spread. J. Virol. **71:**8397–8404.
35. **Mijnes, J. D., L. M. van der Horst, E. van Anken, M. C. Horzinek, P. J. Rottier, and R. J. de Groot.** 1996. Biosynthesis of glycoproteins E and I of

feline herpesvirus: gE-gI interaction is required for intracellular transport. J. Virol. **70:**5466–5475.

36. **Nagashunmugam, T., J. Lubinski, L. Wang, L. T. Goldstein, B. S. Weeks, P. Sundaresan, E. H. Kang, G. Dubin, and H. M. Friedman.** 1998. In vivo immune evasion mediated by the herpes simplex virus type 1 immunoglobulin G Fc receptor. J. Virol. **72:**5351–5359.
37. **Nishikawa, Y., X. Xuan, and H. Otsuka.** 1999. Biosynthesis and interaction of glycoproteins E and I of canine herpesvirus. Virus Res. **61:**11–18.
38. **Nishikawa, Y., X. Xuan, and H. Otsuka.** 1998. Identification and characterization of the glycoprotein E and I genes of canine herpesvirus. Virus Res. **56:**77–92.
39. **Olsen, L. M., T. H. Ch'ng, J. P. Card, and L. W. Enquist.** 2006. Role of pseudorabies virus Us3 protein kinase during neuronal infection. J. Virol. **80:**6387–6398.
40. **Pickard, G. E., C. A. Smeraski, C. C. Tomlinson, B. W. Banfield, J. Kaufman, C. L. Wilcox, L. W. Enquist, and P. J. Sollars.** 2002. Intravitreal injection of the attenuated pseudorabies virus PRV Bartha results in infection of the hamster suprachiasmatic nucleus only by retrograde transsynaptic transport via autonomic circuits. J. Neurosci. **22:**2701–2710.
41. **Polcicova, K., P. S. Biswas, K. Banerjee, T. W. Wisner, B. T. Rouse, and D. C. Johnson.** 2005. Herpes keratitis in the absence of anterograde transport of virus from sensory ganglia to the cornea. Proc. Natl. Acad. Sci. USA **102:** 11462–11467.
42. **Saldanha, C. E., J. Lubinski, C. Martin, T. Nagashunmugam, L. Wang, H. van Der Keyl, R. Tal-Singer, and H. M. Friedman.** 2000. Herpes simplex virus type 1 glycoprotein E domains involved in virus spread and disease. J. Virol. **74:**6712–6719.
43. **Samuel, M. A., H. Wang, V. Siddharthan, J. D. Morrey, and M. S. Diamond.** 2007. Axonal transport mediates West Nile virus entry into the central nervous system and induces acute flaccid paralysis. Proc. Natl. Acad. Sci. USA **104:**17140–17145.
44. **Smeraski, C. A., P. J. Sollars, M. D. Ogilvie, L. W. Enquist, and G. E. Pickard.** 2004. Suprachiasmatic nucleus input to autonomic circuits identified by retrograde transsynaptic transport of pseudorabies virus from the eye. J. Comp. Neurol. **471:**298–313.
45. **Smith, G. A., S. P. Gross, and L. W. Enquist.** 2001. Herpesviruses use bidirectional fast-axonal transport to spread in sensory neurons. Proc. Natl. Acad. Sci. USA **98:**3466–3470.
46. **Snyder, A., K. Polcicova, and D. C. Johnson.** 2008. Herpes simplex virus gE/gI and US9 proteins promote transport of both capsids and virion glycoproteins in neuronal axons. J. Virol. **82:**10613–10624.
47. **Swanson, L. W.** 1992. Brain maps: structure of the rat brain. Elsevier Science, Amsterdam, The Netherlands.
48. **Tirabassi, R. S., and L. W. Enquist.** 2000. Role of the pseudorabies virus gI cytoplasmic domain in neuroinvasion, virulence, and posttranslational N-linked glycosylation. J. Virol. **74:**3505–3516.
49. **Tsujimura, K., T. Yamanaka, T. Kondo, H. Fukushi, and T. Matsumura.** 2006. Pathogenicity and immunogenicity of equine herpesvirus type 1 mutants defective in either gI or gE gene in murine and hamster models. J. Vet. Med. Sci. **68:**1029–1038.
50. **Vernon, S. K., M. Ponce de Leon, G. H. Cohen, R. J. Eisenberg, and B. A. Rubin.** 1981. Morphological components of herpesvirus. III. Localization of herpes simplex virus type 1 nucleocapsid polypeptides by immune electron microscopy. J. Gen. Virol. **54:**39–46.
51. **Wang, F., W. Tang, H. M. McGraw, J. Bennett, L. W. Enquist, and H. M. Friedman.** 2005. Herpes simplex virus type 1 glycoprotein e is required for axonal localization of capsid, tegument, and membrane glycoproteins. J. Virol. **79:**13362–13372.
52. **Whealy, M. E., J. P. Card, A. K. Robbins, J. R. Dubin, H. J. Rziha, and L. W. Enquist.** 1993. Specific pseudorabies virus infection of the rat visual system requires both gI and gp63 glycoproteins. J. Virol. **67:**3786–3797.
53. **Whitbeck, J. C., A. C. Knapp, L. W. Enquist, W. C. Lawrence, and L. J. Bello.** 1996. Synthesis, processing, and oligomerization of bovine herpesvirus 1 gE and gI membrane proteins. J. Virol. **70:**7878–7884.
54. **Zsak, L., F. Zuckermann, N. Sugg, and T. Ben-Porat.** 1992. Glycoprotein gI of pseudorabies virus promotes cell fusion and virus spread via direct cell-to-cell transmission. J. Virol. **66:**2316–2325.